Abnormal Enhancement of N_2^+ Emission Induced by Lower Frequency in N_2 Dual-Frequency Capacitively Coupled Plasmas

2012 Plasma Sci. Technol. 14 222

(http://iopscience.iop.org/1009-0630/14/3/07)

Abnormal Enhancement of N_2^+ Emission Induced by Lower Frequency in N_2 Dual-Frequency Capacitively Coupled Plasmas*

YU Yiqing (虞一青)[1], XIN Yu (辛煜)[1], LU Wenqi (陆文琪)[2], NING Zhaoyuan (宁兆元)[1]

[1]School of Physical Science and Technology, Soochow University, Suzhou 215006, China
[2]School of Physics and Optoelectronic Technology, Dalian University of Technology, Dalian 116024, China

Abstract Nitrogen dual-frequency capacitively coupled plasmas (DF-CCPs) with different frequency configurations, i.e., 60/2 MHz and 60/13.56 MHz, are investigated by means of optical emission spectroscopy (OES) and a floating double probe. The excited nitrogen molecule ion N_2^+(B) is monitored by measuring the emission intensity of the (0,0) bandhead of the first negative system (FNS) at 391.44 nm. It is shown that in the discharge with 60/13.56 MHz, the N_2^+ emission intensity decreases with the increase in pressure. In the discharge with 60/2 MHz, however, an abnormal enhancement of N_2^+ emission at higher pressure is observed when a higher power of 2 MHz is added. Variation in the ion density shows a similar dependence on the gas pressure. This indicates that in the discharge with 60/2 MHz there is a mode transition from the alpha to gamma type when a higher power of 2 MHz is added at high pressures. Combining the measurements using OES and double probe, the influence of low frequency on the discharge is investigated and the excitation route of the N_2^+(B) state in the discharge of 60/2 MHz is also discussed.

Keywords: dual-frequency capacitively coupled plasma, double probe, optical emission spectroscopy

PACS: *52.80.Pi, 52.70.Kz, 52.70.Ds*

DOI: 10.1088/1009-0630/14/3/07

1 Introduction

Low pressure capacitively coupled discharges are widely used in materials processing applications, such as thin film deposition, dielectric etching and photoresist ashing in microelectronic engineering [1]. With the continuous reduction of the critical dimension in ultra-large scale integrated (ULSI) circuits, dual-frequency capacitively coupled plasmas (DF-CCPs) containing nitrogen and fluorocarbon gas [2∼4] were applied to the etching of material, with low dielectric constant and used as an insulating layer. In the etching process, the behavior of ions could be of significant importance in anisotropic etching and control of etching selectivity. In previous studies, more attention was paid to the electron heating mechanism, bulk plasma and sheath properties by using analytic models or numerical simulation techniques [5∼7].

As a simple and noninvasive technique, OES is widely applied in the diagnostics of low pressure plasmas [8]. From the recorded emission spectroscopy, many plasma parameters, such as electron density and temperature [9∼12], could be obtained. In addition, OES also shows versatility in monitoring the behavior of ions or radicals which are of interest in plasma processing. QAYYUM et al. studied the dependence of excited N_2^+ and N_2 states by measuring emission intensities of the bandheads of the first negative and second positive systems [13]. By using OES in Ar/N_2 microwave electron cyclotron resonance discharge, DING et al. [14] studied the effect of gas flow ratio on emitting radicals and the mechanical properties of silicon nitride films. By a comparison of the measured and calculated spectra, HUANG et al. studied frequency dependence of N_2 and N_2^+ rotational and vibrational temperatures in nitrogen capacitively coupled plasmas [15,16]. However, work on the ion behavior in nitrogen DF-CCPs with different frequency configurations has rarely been reported yet.

In this study, the behavior of nitrogen ions is studied by means of OES and double probe in DF-CCPs with two different frequency configurations, i.e., 60/2 MHz and 60/13.56 MHz. It is found that in the nitrogen DF-CCP with 60/2 MHz, an abnormal enhancement of the emission at 391.44 nm occurs at higher pressure when a higher power of 2 MHz is applied. With the ion density measured by a double probe, the excitation mechanism of the emitting N_2^+(B) state is also discussed.

*supported by National Natural Science Foundation of China (Nos. 10635010, 10775103)

2 Experimental setup

A schematic diagram of the experimental setup is shown in Fig. 1. The inner diameter of the reactor vacuum chamber is 300 mm and the diameters of the upper and lower electrodes are 220 mm and 200 mm, respectively. Gap distance between the two parallel electrodes is kept at 45 mm. In the experiment, both the upper and lower cylindrical electrodes are supplied by the radio frequency (RF) sources through an L-type matching box, respectively. The upper electrode is connected to the high frequency (HF) source of 60 MHz while the lower one is powered by the low frequency (LF) source, 2 MHz or 13.56 MHz. A pure nitrogen gas (99.999%) is introduced into the chamber via a mass flow controller.

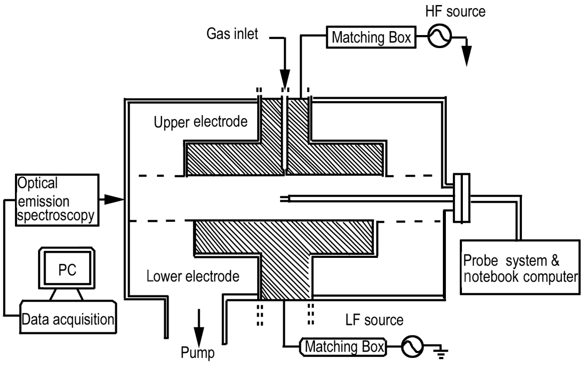

Fig.1 Schematic diagram of the DF-CCP experimental setup

Recently, improved double probe methods and data analysis techniques were developed for the diagnosis of different kinds of plasma discharges [17~19]. A complete floating double probe technique is used in ion density measurement in DF-CCPs with different frequency configurations [20,21]. The double probe system is powered by the notebook computer battery to avoid serious RF perturbation, especially from the LF source of 2 MHz. The probe consists of tungsten tips with a diameter of 0.2 mm and a length of 5 mm. For all measurements the probe tip is located at the radial center of the discharge chamber. The ion density is obtained from standard analysis of the double probe characteristics [22]. With the electron temperature taken from the slope of the double probe I-V characteristic, the ion density n_i can be obtained from the ion saturation current I_i

$$I_i = e n_s u_B A \quad \text{and} \quad n_i \approx \frac{n_s}{0.61}, \tag{1}$$

where e is the electron charge, n_s is the plasma density at the sheath edge, $u_B = (eT_e/M)^{1/2}$ is the Bohm velocity with M the ion mass and A is the probe tip area.

An optical emission spectrometer (AvaSpec-2048FT-8-RM) is used to measure the emission spectrum of the nitrogen discharges. The wavelength resolution of the spectrometer is 0.05 nm to 0.13 nm, with a range of wavelength from 200 nm to 900 nm. During the whole experiment, both the probe and OES fiber are fixed at the same plane 2.5 cm below the upper electrode plane.

3 Results and discussion

The emission spectra of the nitrogen DF-CCP discharges is shown in Fig. 2, with 60/13.56 MHz and 60/2 MHz, as well as a HF and LF power of 100 W and 50 W, respectively. For a simple comparison, the intensities are normalized to the emission of the (1,4) bandhead of the second positive system at 399.84 nm. It can be seen that the intensity of the 391.44 nm emission, (0,0) band of the N_2^+ FNS ($B^2\sum_u^+$-$X^2\sum_g^+$), in the discharge with 60/2 MHz is much higher than that with 60/13.56 MHz. In Fig. 3 a dependence of the emission intensities at 391.44 nm on the pressure in DF-CCPs at a fixed HF power of 100 W with different low frequencies is shown. Regardless of the LF power, the emission intensities decrease with the increase in pressure for the discharge with 60/13.56 MHz. This dependence is similar to that of the ion density, as will be shown below in Fig. 4(a). The large collisional de-excitation cross section of the radiative $N_2^+(B)$ state may also contribute to this decrease [23]. Cases with 60/2 MHz DF-CCP and lower LF power are similar. However, as a higher power of 2 MHz is applied, there is a remarkable enhancement of the N_2^+ emission intensity at 391.44 nm for higher gas pressure.

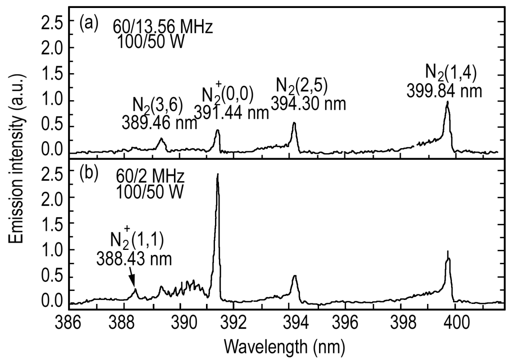

Fig.2 Emission spectra at power of 100/50 W and a gas pressure of 20 Pa for (a) discharge with 60/13.56 MHz and (b) discharge with 60/2 MHz. Intensity is normalized to the emission line at 399.84 nm

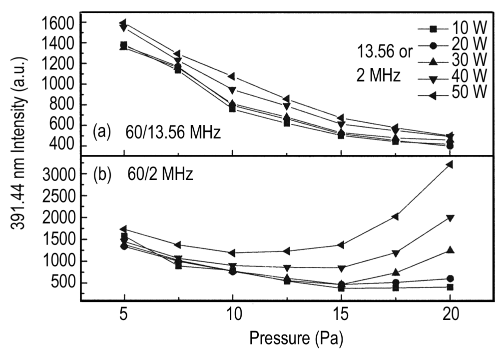

Fig.3 Intensity of (0,0) band of the N_2^+ FNS at 391.44 nm as a function of gas pressure for discharges with (a) 60/13.56 MHz and (b) 60/2 MHz and different LF power. The HF power is kept at 100 W

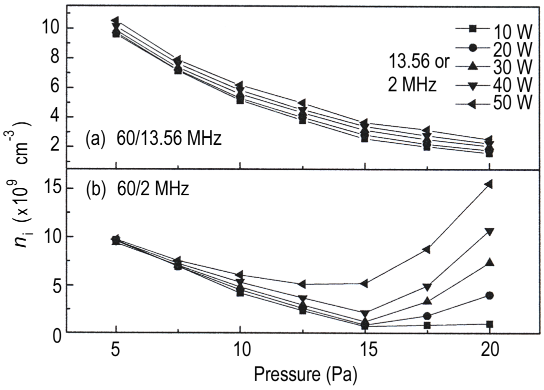

Fig.4 Ion density as a function of gas pressure for discharges with (a) 60/13.56 MHz and (b) 60/2 MHz. The conditions are the same as those in Fig. 3

In Fig. 4(a) nitrogen ion densities measured by double probe in DF-CCPs with 60/13.56 MHz under conditions identical to those in Fig. 3(a) are presented. Since the density of the $N_2^+(B)$ state is much lower than that of $N_2^+(X)$, the probe-measured ion density is mainly contributed by $N_+^2(X)$. Compared to the emission intensity variation shown in Fig. 3(a), it can be seen that there is a similar dependence of the ion density variation with pressure. In general, the electron collision frequency increases with the increase in gas pressure and neutral nitrogen molecule density. The collisional energy loss per electron-ion pair generated, E_c, increases with pressure and this leads to the decrease in ion density with pressure in the discharge with 60/13.56 MHz [1].

However, a substantial increase in the ion density occurs in the discharge with 60/2 MHz at higher gas pressure as larger LF power is applied, which is shown in Fig. 4(b). For example, with pressure kept at 20 Pa, the ion density increases from about 1×10^9 cm^{-3} to 1.6×10^{10} cm^{-3} as the 2 MHz power increases from 10 W to 50 W. This may be attributed to the enhanced ionization near the LF powered electrode, which is a result of stronger secondary electron emission (SEE) induced by strong ion bombardment at higher pressure [24,25].

In the RF capacitive discharge, with an increase in RF voltage, there is a mode transition from the α to γ type [26∼28]. Accompanied by this transition is an abrupt increase in the plasma density [29]. In the nitrogen gas RF capacitive discharges at intermediate pressure, VIDAUD et al. observed the discharge mode transition from α to γ type accompanied by an abrupt increase in the molecular nitrogen ion emission [30], which is similar to that shown in Fig. 3. Similarly, different modes also exist in low pressure hydrogen DF capacitive discharges with 27/2 MHz. It is found that when the LF voltage exceeds some critical value the DF discharge turns from the first mode to the second one [31]. In our discharge with 60/2 MHz a similar transition could occur when a high LF power is applied at high gas pressure.

Generally for the same input power, the mean sheath potential over the electrode for 2 MHz is higher than that for 13.56 MHz. In addition, the ion energy distribution in DF-CCP with 2 MHz is also wider. Thus in the DF discharge with 60/2 MHz, SEE induced by energetic ion bombardment is stronger than that in the discharge with 60/13.56 MHz. The effective multiplication of secondary electrons could contribute to the nitrogen molecule ionization process, especially at higher gas pressure. LISOVSKIY et al. also pointed out that at lower pressure the near-electrode sheath is not broken down and the sheaths serve as a source of fast electrons [28]. DONKÓ et al. [25] studied the effect of secondary electrons on DF argon discharge by using particle-in-cell simulation. When considering SEE in the DF discharge, they found that the plasma density and ion flux onto the electrode increase sharply with the applied low frequency voltage at a high gas pressure. A similar situation could be expected in our nitrogen plasmas with 60/2 MHz, especially at higher pressures and higher LF power.

Based on the OES and probe measurement, the excitation route of the $N_2^+(B)$ state could be explained. For a selected transition, the emission intensity is proportional to the population density of the upper radiative state. Therefore, an increase in the N_2^+ FNS emission at higher pressure in the discharge with 60/2 MHz indicates the increase in density of $N_2^+(B)$. In low pressure discharges, the $N_2^+(B)$ state is essentially populated by electronic excitation processes [12,13]

$$e + N_2(X) \rightarrow 2e + N_2^+(B), \tag{2}$$

$$e + N_2^+(X) \rightarrow e + N_2^+(B). \tag{3}$$

For a given excited state, its population and depopulation processes will be balanced in a steady-state discharge. The emission intensity of the FNS is contributed by the two mechanisms, presented in Eqs. (2) and (3). In these two electron impact excitation processes, a higher excitation rate coefficient means more contribution to the generation of $N_2^+(B)$ [12]. The rate coefficient of electron impact excitation is calculated as

$$k = \int_{E_{\rm th}}^{\infty} \sigma(E)\sqrt{\frac{2E}{m_{\rm e}}} f(E){\rm d}E, \tag{4}$$

where σ, E and m_e are cross sections of electron impact excitation, electron kinetic energy and mass, respectively [9,10]. $E_{\rm th}$ is the threshold energy for the electronic excitation and $f(E)$ is the electron energy distribution function (EEDF) which could be normalized as $\int_0^\infty f(E){\rm d}E = 1$.

Electron impact excitation cross sections of $N_2^+(B)$ from ground state nitrogen molecule $N_2(X)$ and ground state molecule ion $N_2^+(X)$ are compiled by TABATA et al. [32]. The direct excitation threshold energy from the $N_2(X)$ to $N_2^+(B)$ state is about 18.8 eV, much higher than that from $N_2^+(X)$, 3.17 eV. Moreover, the electronic excitation cross section of reaction (3) remains several times, or even an order of magnitude larger than that of reaction (2), especially at lower electron energy.

With an electron temperature range of 1 eV to 7 eV in typical low pressure RF discharges, the rate coefficients of the two electronic excitation processes are calculated according to Eq. (4). During the calculation, the above cross sections are used and a Maxwellian electron distribution is assumed. It is shown in Fig. 5 that both rate coefficients increase with the electron temperature. For example, the rate coefficient of excitation from N_2^+(X) to N_2^+(B) increases from 3.1×10^{-9} cm^3/s at 1 eV to about 2.5×10^{-8} cm^3/s at 7 eV. While the corresponding coefficient from N_2(X) to N_2^+(B) increases from 6×10^{-18} cm^3/s to about 2.2×10^{-10} cm^3/s. The former coefficient always keeps two orders of magnitude higher than the latter one, even at the high electron temperature limit. Though the electron energy distribution often deviates from the Maxwellian, the number of electrons with lower energy greatly exceeds those in the high energy tail of the EEDF [24,33~35]. Thus the above discussion still holds for a non-Maxwellian electron distribution.

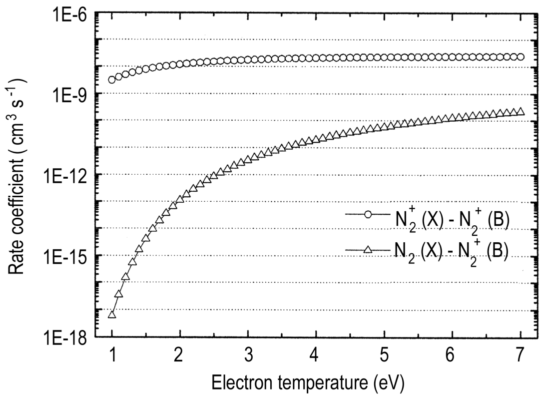

Fig.5 Dependence of the rate coefficients of two electronic excitations on electron temperature

As is mentioned, the rate coefficient k of electronic excitation from N_2^+(X) is much larger than that from N_2(X). Thus considering the two excitation rate coefficients together with the ion density measured by the double probe, it can be concluded reasonably that the increase in N_2^+(X) and then its subsequent electronic excitation to N_2^+(B) account for the abnormal enhancement of the N_2^+ FNS emission.

4 Conclusion

The influence of different low frequencies on the N_2^+ behavior in the nitrogen DF-CCPs with 60/2 MHz and 60/13.56 MHz is studied by using OES and a floating double probe. In DF-CCP with 13.56 MHz as the LF source, the N_2^+(B) emission at 391.44 nm decreases with the increase in pressure. At higher pressure and a higher power of 2 MHz, however, a substantial increase in N_2^+ FNS emission occurs. The probe-measured nitrogen molecule ion density shows a similar dependence with that of the emission spectra. A remarkable enhancement of nitrogen molecule ion density in the discharge with 60/2 MHz at higher pressure is attributed to the stronger ionization of SEE which is induced by energetic ion bombardment. An abrupt growth of the ion density and the molecular ion emission indicates the transition of the discharge from α to γ type. The enhancement of N_2^+ FNS emission at a high gas pressure is mainly through the electronic excitation of the N_2^+(X) state when a higher LF power is applied in the discharge with 60/2 MHz.

References

1 Lieberman M A, Lichtenberg A J, 2005, Principles of Plasma Discharges and Materials Processing. Wiley, Hoboken, New Jersey. p.1,81
2 Ishikawa K, Yamaoka Y, Nakamura M, et al. 2006, J. Appl. Phys., 99: 083305
3 Uchida S, Takashima S, Hori M, et al. 2008, J. Appl. Phys., 103: 073303
4 Xu Y J, Ye C, Huang X J, et al. 2008, Chin. Phys. Lett., 25: 2942
5 Boyle P C, Ellingboe A R, Turner M M. 2004, J. Phys. D: Appl. Phys., 37: 697
6 Kim H C, Lee J K, Shon J W. 2003, Phys. Plasmas, 10: 4545
7 Jiang W, Mao M, Wang Y N. 2006, Phys. Plasmas, 13: 113502
8 Fantz U. 2006, Plasma Sources Sci. Technol., 15: S137
9 Zhu X M, Pu Y K. 2006, Phys. Plasmas, 13: 063507
10 Donnelly V M. 2004, J. Phys. D: Appl. Phys., 37: R217
11 Qayyum A, Zeb S, Naveed M A, et al. 2007, J. Quant. Spectrosc. Radiat. Transfer, 107: 361
12 Isola L M, Gómez B J, Guerra V. 2010, J. Phys. D: Appl. Phys., 43: 015202
13 Qayyum A, Zeb S, Naveed M A, et al. 2005, J. Appl. Phys., 98: 103303
14 Ding W Y, Xu J, Lu W Q, et al. 2009, Phys. Plasmas, 16: 053502
15 Huang X J, Xin Y, Yuan Q H, et al. 2008, Phys. Plasmas, 15: 073501
16 Huang X J, Xin Y, Zhang J, et al. 2009, Chin. Phys. Lett., 26: 055202
17 Smith B A and Overzet L J. 1999, Plasma Sources Sci. Technol., 9: 82
18 Kubo T, Kawata H, Murata K. 1998, Rev. Sci. Instrum., 69: 2681
19 Ghim Y C and Hershkowitz N. 2009, Rev. Sci. Instrum., 80: 033502
20 Bi Z H, Xu X, Liu Y X, et al. 2011, Plasma Sci. Technol., 13: 181
21 Jiang X Z, Liu Y X, Yang S, et al. 2011, J. Vac. Sci. Technol. A, 29: 011006
22 Chen F F. 1965, Electric Probes in Plasma Diagnostic Techniques. edited by Huddlestone R H and Leonard S L. Academic Press, New York. p.150,183
23 Phillips D M. 1975, J. Phys. D: Appl. Phys., 8: 507
24 Ahn S K, Chang H Y. 2009, Appl. Phys. Lett., 95: 111502

25 Donkó Z, Schulze J, Hartmann P, et al. 2010, Appl. Phys. Lett., 97: 081501.

26 Lisovskiy V A, Yegorenkov V D. 2004, Vacuum, 74: 19

27 Belenguer P and Boeuf J P. 1990, Phys. Rev. A, 41, 4447

28 Lisovskiy V, Booth J P, Landry K, et al. 2006, Phys. Plasmas, 13: 103505

29 Godyak V A and Khanneh A S. 1986, IEEE Trans. Plasma Sci., PS-14: 112

30 Vidaud P, Durrani S M A, Hall D R. 1988, J. Phys. D: Appl. Phys., 21, 57

31 Lisovskiy V, Booth J P, Landry K, et al. 2008, Plasma Sources Sci. Technol., 17: 025002

32 Tabata T, Shirai T, Sataka M, et al. 2006, At. Data Nucl. Data Tables, 92: 375

33 Godyak V A, Piejak R B, Alexandrovich B M. 1992, Plasma Sources Sci. Technol., 1: 36

34 Ferreira C M, Loureiro J. 2000, Plasma Sources Sci. Technol., 9: 528

35 Fattah E A, Sugai H. 2003, Appl. Phys. Lett., 83: 1533

(Manuscript received 9 March 2011)
(Manuscript accepted 14 July 2011)
E-mail address of corresponding author XIN Yu:
xylzf_1999@suda.edu.cn